DOI: 10.13009/EUCASS2022-6152
9TH EUROPEAN CONFERENCE FOR AERONAUTICS AND SPACE SCIENCES (EUCASS)

Linear dynamical model of overexpanded supersonic jet resonances

V. Jaunet G. Lehnasch E. Goncalves

ISAE-ENSMA, Institut PPrime, Université de Poitiers,
UPR-3346 CNRS Poitiers, France
vincent.jaunet@ensma.fr

1. Introduction

Resonances in jet flows, issued from "truncated ideal contour" (TIC) nozzle and evolving in free separation regime, have been observed in very narrow ranges of over-expansion ratio (Jaunet et al., 2017, Martelli et al., 2020). Recent studies have shown that the associated pressure disturbances are likely to induce intense lateral forces that may cause structural damages or even flight control issues (Bakulu et al., 2021). At these regimes, the presence of Mach disks in

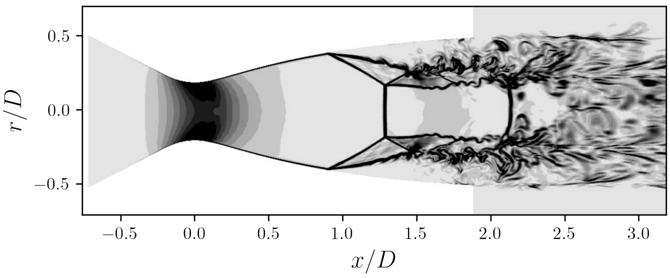

Figure 1: Pseudo-Schlieren visualization of TIC nozzle jet in Free Separated Separation (FSS) regime.

the flow slows down the core of the flow, while a higher velocity annular flow surrounds this slower core, as illustrated in figure 1. The flow is hence made of two annular mixing layers (ML), that have been shown to be of importance in the resonance mechanism. To the best of our knowledge, no model has been yet proposed to predict the occurrence of resonances in these flows. Following recent studies on screeching jets (Edgington-Mitchell et al., 2018, Mancinelli et al., 2019, Nogueira et al., 2021), we propose to explore the possible mechanisms of resonance with the help of a simplified linear dynamical model of the flow, built from numerical data available. The influence of the internal mixing layer position is more particularly evaluated.

2. Linear model

We propose to use an approach similar to the one followed by Mancinelli et al. (2019) and Mancinelli et al. (2021). It consists in modelling the supersonic jet dynamics using locally-parallel linear stability theory. In the following, all variables are normalised by the fully expanded jet diameter D_j, the ambient density ρ_∞ and ambient speed of sound c_∞. The Reynolds decomposition, is applied to the flow-state vector $\underline{q'}$ of primitive variables, where the mean and fluctuating components are $\overline{q}$ and q, respectively. In the following, $\overline{\rho}$, $\overline{T}$ and $\overline{u_x}$ thus represent the mean density, temperature and streamwise velocity fields of the base flow at a selected streamwise position. Assuming a normal-mode ansatz in all directions except the radius and linearizing the Euler equations around this base flow, we obtain the compressible Rayleigh equation for the pressure disturbances, that is being solved for:

$$\frac{\partial^2 \hat{p}}{\partial r^2} + \left(\frac{1}{r} - \frac{2k}{\overline{u}_x k - \omega} \frac{\partial \overline{u}_x}{\partial r} - \frac{\gamma - 1}{\gamma \overline{\rho}} \frac{\partial \overline{\rho}}{\partial r} + \frac{1}{\gamma \overline{T}} \frac{\partial \overline{T}}{\partial r} \right) \frac{\partial \hat{p}}{\partial r} - \left(k^2 + \frac{m^2}{r^2} - \frac{(\overline{u}_x k - \omega)^2}{(\gamma - 1)\overline{T}} \right) \hat{p} = 0, \quad (1)$$

DOI: 10.13009/EUCASS2022-6152

where γ is the specific heat ratio for a perfect gas, k is the streamwise wavenumber and m is the azimuthal wavenumber. Note, that in the following, we will focus exclusively on the $m = 1$ non-axisymmetric mode that is the only one related to the generation of lateral forces. The non-dimensional pulsation $\omega = 2\pi St M_a$ is computed via the acoustic Mach number of the jet $M_a = U_j/c_\infty$, where U_j is the equivalent fully expanded velocity of the flow, and $St = fD_j/U_j$ the Strouhal number of the flow.

The solution of the linear stability problem is obtained by specifying a real or complex frequency ω and by solving the resulting augmented eigenvalue problem $k = k(\omega)$, with $\hat{p}(r)$ the associated pressure eigenfunction. The eigenvalue problem is solved numerically by discretizing the Rayleigh equation in the radial direction using Chebyshev polynomials. A mapping function is used to non-uniformly distribute the grid points and refine the region where shear is more important (Trefethen, 2000).

3. Parallel flow assumption

As the nozzle pressure ratio increases, the mean flow structure varies greatly: the strength of the Mach disk increases with the Nozzle Pressure Ratio (NPR), the relative position of the MLs changes, following the modifications of the shock cells structure, and their relative thicknesses may also vary. Hence, the whole exhaust jet dynamics may be impacted by these changes in mean flow and that may explain why resonances in C-D nozzle arise at very specific NPRs. For this purpose, we propose in this paragraph to evaluate the importance of some of these flow features on the dynamics of the flow.

3.1 Base flow parametrization

As can be seen in figure 2, the mean flow profiles downstream of the first Mach disk, are, as expected, composed of two MLs: one separating the supersonic flow and the ambient, the other one separating the subsonic core and the supersonic flow.

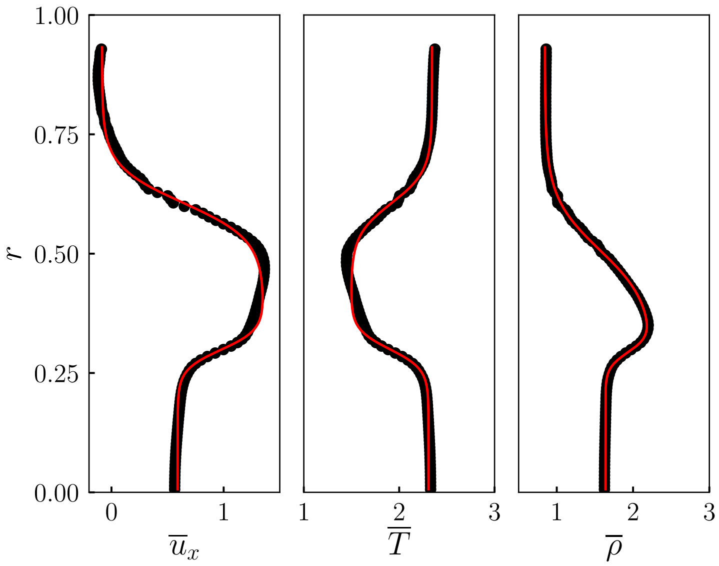

Figure 2: Typical base flow used for the study of local stability properties of the flow. The considered profiles are extracted at the distance from the throat $x/D = 1.6$ (where D is the exit nozzle diameter), in between the two first Mach disks of the flow. Dots represent the numerical data and red lines are the fitted analytical functions.

A representative analytical formulation of the base flow is obtained through a regression of the numerical data available (DDES simulation previously done in Bakulu et al. (2021) with the following analytical profiles:

$$
\begin{aligned}
q_{in}(r) &= q_i \left[1 - \left(1 - \frac{q_a}{q_i}\right)\left(1 + \tanh\left(\frac{r - R_i}{b_i}\right)\right)\right] \\
q_{out}(r) &= 1 - \frac{1}{2}\left(1 - \frac{q_e}{q_a}\right)\left(1 + \tanh\left(\frac{r - R_e}{b_e}\right)\right) \\
q(r) &= q_{in}(r) \times q_{out}(r),
\end{aligned} \tag{2}
$$

DOI: 10.13009/EUCASS2022-6152

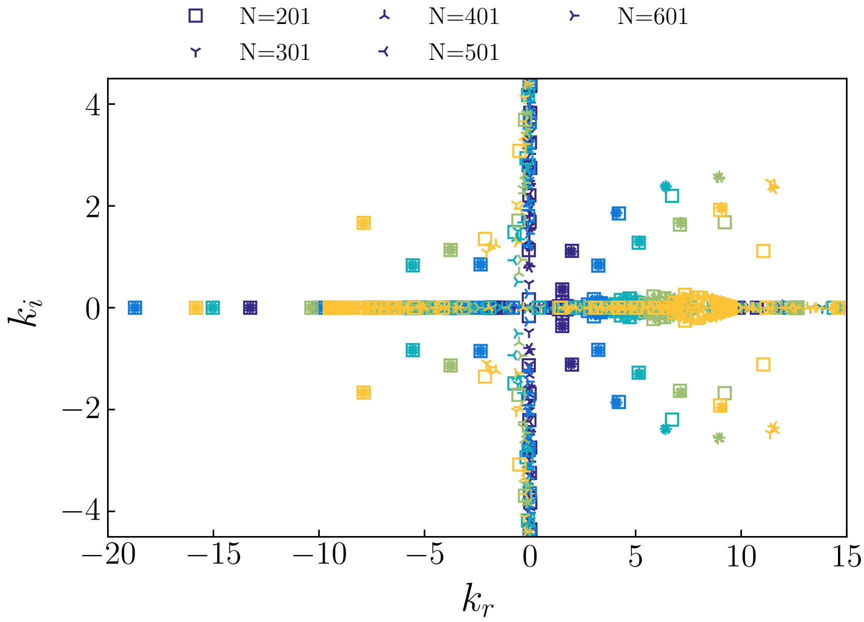

Figure 3: Convergence of the eigenvalue spectrum with respect to the number of Chebychev collocation points and Strouhal number from 0.1 (blue) to 0.5 (yellow).

where q here stands for M, $r\bar{h}o$ or $\bar{T}$. The indices i, a, and e respectively refer to the inner, the annular and the external flow variable of interest. (R_i, b_i),(R_e, b_e) the inner and external ML radial positions and thicknesses, respectively.The optimal analytical profiles are compared with the reference numerical data in figure 2, showing a satisfactory agreement.

3.2 Convergence study

We present in figure 3 the convergence of the eigenvalue spectrum with respect to the number of Chebychev collocation points N and the Strouhal number. As can be seen, the convergence is more difficult to reach at high frequencies, especially for the Kelvin-Helmholtz modes (the isolated modes in the right lower quarter of the figure), but the spectrum seems converged above $N = 301$ points. Therefore, a total number of $N = 401$ collocation points is used for all the computations in this study.

3.3 Variation of the radial position of the inner mixing layer

The influence of the relative position of the MLs are first studied by assuming constant internal reference u_x level. We perform linear stability analyses on base flows with varying inner ML positions as presented in figure 4. The inner, annular and external Mach number were chosen to match approximately the numerical simulations downstream of the first Mach disk: $M_i = 0.6$, $M_a = 1.4$ and $M_e = 0$. The density profile was computed using the Crocco-Busemann relation (**?**). A total number of 36 base flows were used to finely study the change in the corresponding linear dynamics.

Typical eigenspectra obtained at $St = 0.2$ and $m = 1$ are presented in figure 5. We recognize on the right hand side of the figure, *i.e.* for $k_r > 0$ two unstable eigenvalues corresponding to the Kelvin-Helmholtz (K-H) modes of both the inner and outer MLs. The least unstable being the K-H mode associated to the inner ML. The continuous acoustic branch is clearly visible with a relatively weak influence of R_i on the *locii* of the corresponding modes. Propagative and evanescent trapped waves wavenumbers (Towne et al., 2017) can be identified in $k_r < 0$ plane. Hence, the annular supersonic jets seem to show the same features as a classical top-hat supersonic one. We will focus in the following in extracting the effect of the inner ML position on the characteristics of these waves.

3.3.1 Kelvin-Helmholtz mode

In figure 6, we plot the growth rate evolution of both K-H modes as a function of R_i for various Strouhal numbers. The outer K-H mode is always more unstable that the inner one for all the configurations investigated in this study. This

DOI: 10.13009/EUCASS2022-6152

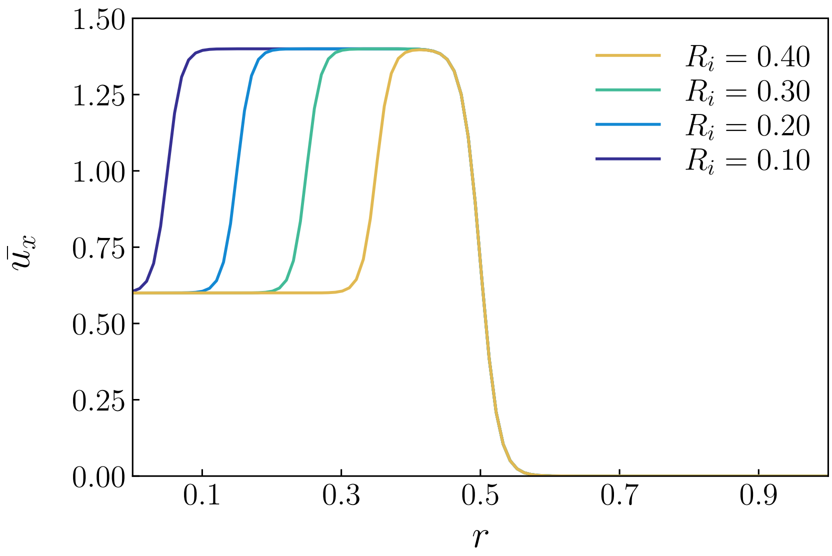

Figure 4: Base flows used to study the effect of the position of the inner mixing layer on the dynamics of the flow.

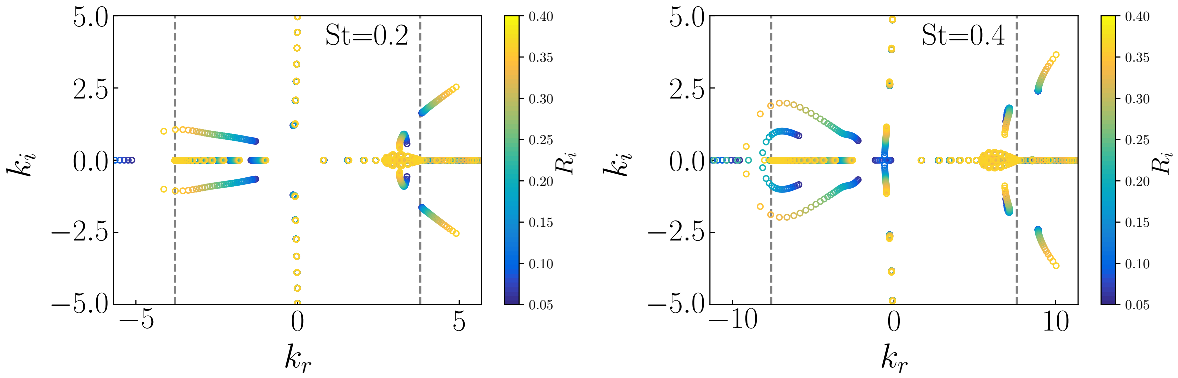

Figure 5: Eigenspectra computed at $St = 0.2$ and $St = 0.4$ for various R_i. The dashed lines indicates the wavenumber corresponding to sonic phase speed.

makes sense considering the fact that the velocity gradient is stronger for the outer ML than for the inner one. The outer mode is all the more unstable that R_i is large, although at high frequencies its growth rate shows a plateau at low values of R_i. On the other hand, the inner ML instability shows an optimal growth rate at specific R_i. This trend shows that there may exist specific base flows and frequencies where the inner and the outer K-H modes possess equivalent growth rate. In some cases, the inner one can even become more unstable than the outer one. However, this may happen at rather high frequencies and might not be relevant for our initial nozzle flow problem for which resonance at lower frequencies are observed.

The pressure eigenfunctions associated with the two identified K-H modes are presented in figure 7 for $St = 0.2$. As expected, the eigenfunction is maximum at the ML location and is zero at the centreline since we focused on the $m = 1$ anti-symmetric wavenumber. The outer K-H mode does not seem to be significantly affected by the inner ML, contrary to the inner one, whose support spreads all the more through the outer mixing layer and above, as both MLs get closer. Interestingly, the radial support of the inner K-H wave decays less rapidly than the outer one which makes possible to detect it quite far away from the jet and allows it to exchange energy with feedback waves outside of the supersonic annular region. This is well in line with the observations of Bakulu et al. (2021) who found the inner mixing layer to be the support of the most of the perturbations associated to the resonance process in their flow.

DOI: 10.13009/EUCASS2022-6152

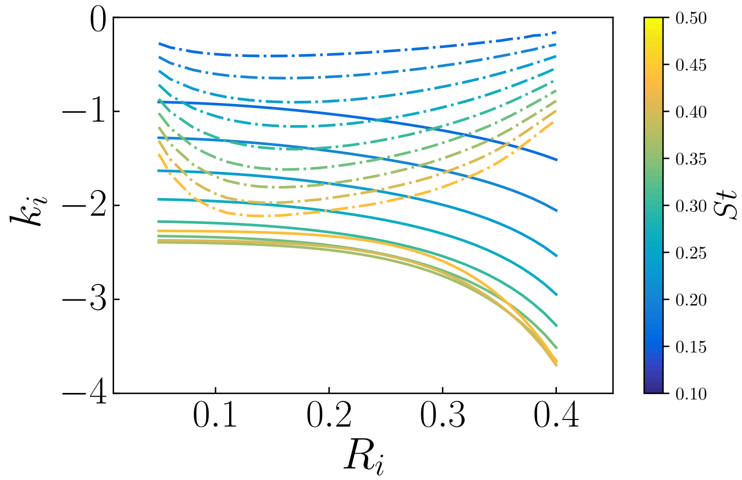

Figure 6: Growth rate of the Kelvin-Helmholtz mode as a function of of Strouhal number and inner ML location R_i. Dashed lines and plain lines corresponds to the inner and outer K-H modes, respectively.

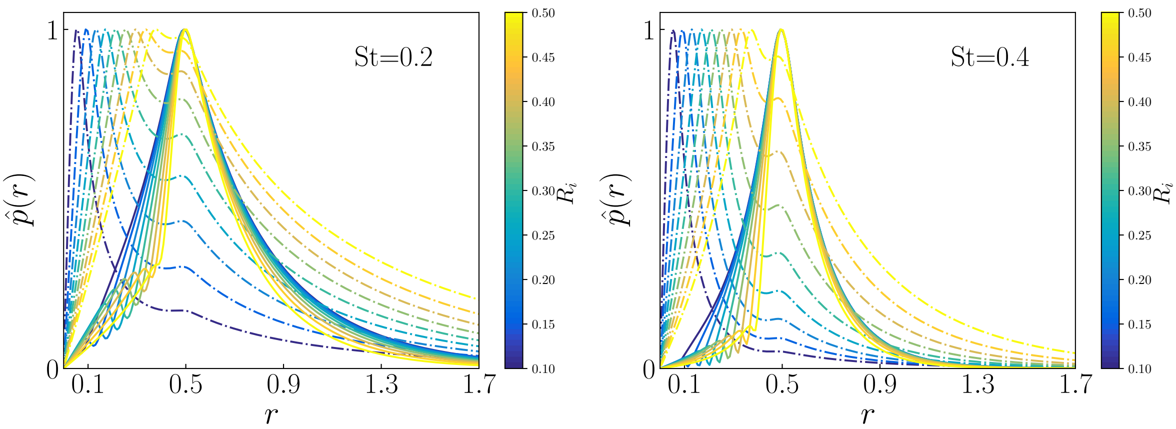

Figure 7: Eigenfunctions associated with the inner (dashed) and outer (plain) K-H modes, normalized with respect to their maximum value, for $St = 0.2$ and $St = 0.4$.

3.3.2 Trapped neutral modes

Neutral waves, trapped by the jet (Towne et al., 2017), have been shown to play a tremendous role in resonance of screeching and impinging jets (see for example Edgington-Mitchell et al. (2018), Gojon et al. (2018), Mancinelli et al. (2021), **?**). Their dispersion relation is a key characteristics that explains cut-on and cut-off frequencies, switching from axisymmetric to helical modes and improves the model predictions (Mancinelli et al., 2019, 2021, Nogueira et al., 2021). Their eigenvalue sits on the real axis of the spectra until they become evanescent. At supersonic speed, jets support both upstream and downstream propagative modes. The upstream propagative one carries energy in the upstream direction. Figure 5 shows that the annular jet configuration, as encountered in the exhaust of over-expanded CD nozzles, also supports such kind of guided, trapped, neutral waves. The dispersion relation of these waves is plotted in figure 8 in the $St - k_r$ plane for various positions of the inner ML.

As expected, at each R_i the neutral waves form a families of modes hierarchically ordered by their radial supports: the higher the frequency, the higher the radial order (*i.e.* the number of nodes and anti-nodes, see Tam and Hu (1989)). As can be seen, the position of the inner ML has a strong impact on the neutral modes dispersion relation: as R_i increases the frequencies at which the modes are encountered also increases. Furthermore, the group velocity of the k_p^+ mode decreases with R_i. This can be understood by recognizing that for $R_i = 0$ or $R_i = R_e$, the base flow is close to a supersonic top-hat jet or a subsonic one respectively. Therefore, the neutral modes behavior seems to vary in between what is expected for subsonic and supersonic jets. Moreover, we see that R_i impacts the domain of existence of the upstream propagating neutral modes. Two main observations can be done. First, the domain where $d\omega/dk < 0$ shifts

DOI: 10.13009/EUCASS2022-6152

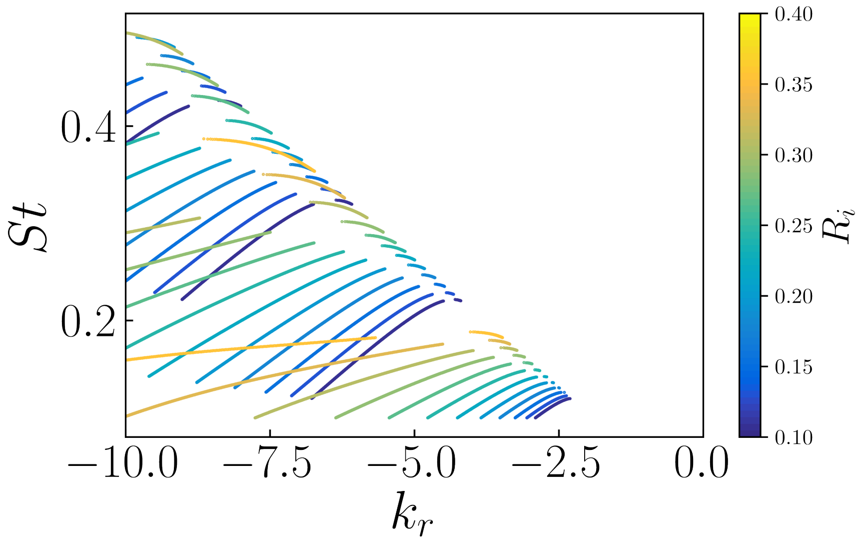

Figure 8: Neutral modes dispersion relation for various positions of the inner mixing layer.

towards higher Strouhal number with increasing R_i. Then, the range of Strouhal number where these neutral modes are encountered significantly varies with Ri.

The eigenfunctions associated with the upstream propagative neutral modes are presented in figure 9. As expected, the radial supports of these modes share common features with Bessel functions. At low Strouhal number the eigenfunctions show one anti-node, whereas for higher frequencies more anti-nodes can be seen. Surprisingly, very little change of the radial support is observed for varying *Ri*. This is due to the fact that these modes are duct-like modes, hence their support being mostly independent of the base flow, contrary to their wavenumber. It is of importance to notice that they also have support outside the jet, as the inner K-H wave, allowing these waves to interact and the upstream mode to carry energy upstream to close a possible feedback loop.

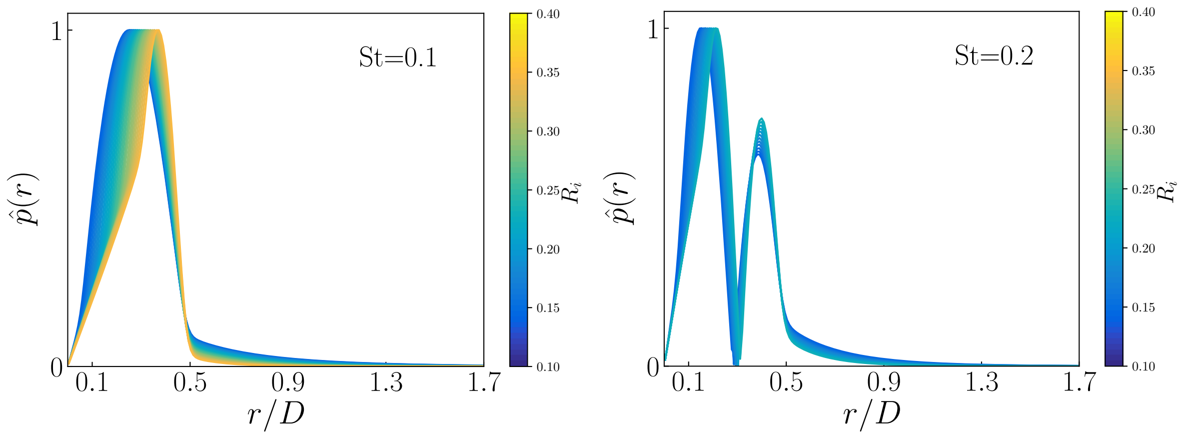

Figure 9: Eigenfunctions associated with the upstream propagative neutral mode, normalized with respect to their maximum value, for $St = 0.1$ and $St = 0.2$.

4. Conclusions and perspectives

The dynamics of an annular over-expanded jet flow issued from a convergent-divergent nozzle operating in free separation regime does not significantly differ from more canonical situations of slightly under-expanded jets. The annular jets support both KH waves and trapped neutral waves, which are necessary ingredients for a jet to undergo resonance. The influence of the relative position of the internal mixing layer was discussed and it was found that it has a strong impact on the supported waves characteristics. Hence, we may infer that there exits specific NPR for which the mean

DOI: 10.13009/EUCASS2022-6152

flow topology of the exhaust flow of a TIC nozzle (*i.e.* Mach disk size, external jet diameter...) is more suitable for resonance to occur than others. Given the sensitivity of the stability waves characteristics observed in this study, modelling possible resonances in annular jets, as recently done in screeching jets (Edgington-Mitchell et al. (2018), Mancinelli et al. (2019, 2021)), will be more complicated for the latter as it involves more parameters. Therefore, we suggest that a parametric stability study of other important flow parameters, such as Mach number (NPR), stagnation temperature, shear layer thickness, should be performed to clarify further why some resonances may only exist in a limited range of nozzle pressure ratio, as observed in Jaunet et al. (2017).

References

F. Bakulu, G. Lehnasch, V. Jaunet, E. Goncalves da Silva, and S. Girard. Jet resonance in truncated ideally contoured nozzles. *Journal of Fluid Mechanics*, 919:A32, 2021. doi: 10.1017/jfm.2021.351.

D. Edgington-Mitchell, V. Jaunet, P. Jordan, A. Towne, J. Soria, and D. Honnery. Upstream-travelling acoustic jet modes as a closure mechanism for screech. *Journal of Fluid Mechanics*, 855, 2018.

R. Gojon, C. Bogey, and M. Mihaescu. Oscillation modes in screeching jets. *AIAA Journal*, 56(7):2918–2924, 2018. URL `https://doi.org/10.2514/1.J056936`.

V. Jaunet, S. Arbos, G. Lehnasch, and S. Girard. Wall pressure and external velocity field relation in overexpanded supersonic jets. *AIAA Journal*, pages 4245–4257, 2017.

M. Mancinelli, V. Jaunet, P. Jordan, and A. Towne. Screech-tone prediction using upstream-travelling jet modes. *Experiments in Fluids*, 60(1):22, 2019.

M. Mancinelli, V. Jaunet, P. Jordan, and A. Towne. A complex-valued resonance model for axisymmetric screech tones in supersonic jets. *Journal of Fluid Mechanics*, 928, 2021.

E. Martelli, L. Saccoccio, P. Ciottoli, C. Tinney, W. J. Baars, and M. Bernardini. Flow dynamics and wall-pressure signatures in a high-reynolds-number overexpanded nozzle with free shock separation. *Journal of Fluid Mechanics*, 895, 2020. URL `https://doi.org/10.1017/jfm.2020.280`.

P. A. Nogueira, P. Jordan, V. Jaunet, A. V. Cavalieri, A. Towne, and D. Edgington-Mitchell. Absolute instability in shock-containing jets. *arXiv preprint arXiv:2106.12690*, 2021.

C. K. W. Tam and F. Q. Hu. On the three families of instability waves of high-speed jets. *Journal of Fluid Mechanics*, 201:447–483, 1989.

A. Towne, A. V. Cavalieri, P. Jordan, T. Colonius, O. Schmidt, V. Jaunet, and G. A. Brès. Acoustic resonance in the potential core of subsonic jets. *Journal of Fluid Mechanics*, 825:1113–1152, 2017.

L. N. Trefethen. *Spectral methods in MATLAB*. SIAM, 2000.